

Energy Technology

Generation, Conversion, Storage, Distribution

Postfach 10 11 61
69451 Weinheim
Germany
Courier services:
Boschstraße 12
69469 Weinheim
Germany
Tel.: (+49) 6201 606 125
E-mail: energy-technology@wiley-vch.de

WILEY-VCH

Dear Author,

Please correct your galley proofs carefully and return them no more than four days after the page proofs have been received.

Please limit corrections to errors already in the text; cost incurred for any further changes or additions will be charged to the author, unless such changes have been agreed upon by the editor.

The editors reserve the right to publish your article without your corrections if the proofs do not arrive in time.

Note that the author is liable for damages arising from incorrect statements, including misprints.

Please note any queries that require your attention. These are indicated with a Q in the PDF and a question at the end of the document.

Reprints may be ordered by filling out the accompanying form.

Return the reprint order form by e-mail with the corrected proofs to Wiley-VCH: energy-technology@wiley-vch.de

To avoid commonly occurring errors, **please ensure that the following important items are correct** in your proofs (please note that once your article is published online, no further corrections can be made):

- **Names** of all authors present and spelled correctly
- **Addresses** and **postcodes** correct
- **E-mail address** of corresponding author correct (current email address)
- **Funding bodies** included and grant numbers accurate
- **Title** of article OK
- All **figures** included
- **Equations** correct (symbols and sub/superscripts)

Corrections should be made directly in the PDF file using the PDF annotation tools. If you have questions about this, please contact the editorial office. The corrected PDF and any accompanying files should be uploaded to the journal's Editorial Manager site.

AUTHOR QUERY FORM

WILEY-VCH

JOURNAL: ENERGY TECHNOLOGY

Article: ente.202100520

Dear Author,

During the copyediting of your manuscript the following queries arose.

Please refer to the query reference callout numbers in the page proofs and respond to each by marking the necessary comments using the PDF annotation tools.

Please remember illegible or unclear comments and corrections may delay publication.

Many thanks for your assistance.

Query No.	Query	Remark
Q-license	<p>Please note that the article can only be published once an appropriate license agreement has been signed. The responsible corresponding author will have received an e-mail invitation to register/log in and sign a license agreement in Wiley Author Services (https://authorservices.wiley.com).</p> <p>The costs of publishing this manuscript OnlineOpen might be covered by one of Wiley's national agreements. To find out more please visit, https://authorservices.wiley.com/author-resources/Journal-Authors/open-access/affiliation-policies-payments/index.html. Eligibility for fee coverage is determined by the affiliation of the responsible corresponding author</p>	
Q1	Please confirm that forenames/given names (blue) and surnames/family names (vermilion) have been identified correctly.	
Q2	As per journal style, C has been changed to italic to maintain consistency in the text and C in subscript has been changed to Roman throughout the article. Please check and confirm.	
Q3	Please provide the expansions of the abbreviations RF and LCD.	
Q4	Please check all equations have been correctly typeset.	
Q5	Please add an acknowledgements section for information regarding funding, etc., if applicable.	

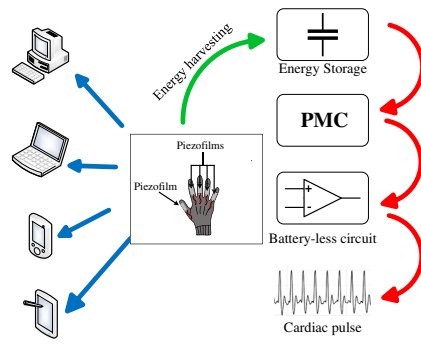
Author: Please confirm that Funding Information has been identified correctly.

Please confirm that the funding sponsor list below was correctly extracted from your article: that it includes all funders and that the text has been matched to the correct FundRef Registry organization names. If a name was not found in the FundRef registry, it may not be the canonical name form, it may be a program name rather than an organization name, or it may be an organization not yet included in FundRef Registry. If you know of another name form or a parent organization name for a "not found" item on this list below, please share that information.

FundRef Name	FundRef Organization Name
--------------	---------------------------

1 **RESEARCH ARTICLES**

2
3 O. Mendez-Lira, E. M. Spinelli,
4 R. Gonzalez-Landaeta* 2100520
5 **Battery-Less Power Management Circuit**
6 **Powered by a Wearable Piezoelectric**
7 **Energy Harvester**



1 The wearable system proposed herein can
2 harvest and manage the energy from daily
3 activities like using a laptop, computer,
4 cellular phone, or tablet. The energy can be
5 used to supply low-power circuits; in our
6 case, the proposed system is tested by
7 detecting the cardiac pulse for 20 s with
8 no batteries, in a comfortable and user-
9 friendly way.

UNCORRECTED PROOF

Battery-Less Power Management Circuit Powered by a Wearable Piezoelectric Energy Harvester

Omar Mendez-Lira, Enrique Mario Spinelli, and Rafael Gonzalez-Landaeta*

A system that aims to manage the energy harvested from the finger movement using a glove-type garment is proposed. For this, five polyvinylidene difluoride (PVDF) film-type sensors are mounted on different interphalangeal joints of the fingers. A 68 $\mu\text{F}/25\text{ V}$ ceramic capacitor is used as a storage device. A battery-less power management circuit (PMC) is proposed to isolate the capacitor from the load to reduce the current consumption while charging. When the voltage across the capacitor reaches a threshold voltage, the user decides when to transfer the energy to the electronic load. To test the proposed system, the harvested and conditioned energy is used to power both the PMC and a battery-less cardiac pulse detection circuit, achieving an autonomy of 20 s. This time depends on the voltage stored in the capacitor and the current consumption of the load. Using the proposed wearable system, it is possible to store up to 700 μJ in the capacitor when a subject manipulates a computer or a cellular phone for 10 min. The proposed system is not limited to the activities presented herein because it can harvest the biomechanical energy from any activity that involves finger movements.

1. Introduction

The need for providing a continuous amount of energy is one of the main concerns in wearable devices.^[1,2] The limited power source (typically rechargeable batteries) has a direct impact on the size, weight, lifetime, and maintenance of the device.^[3] To tackle this, some authors have proposed different approaches like using energy harvesting (EH) for wearable devices to reduce the use of batteries or even replace them.^[4]

EH systems transform nonelectric energy from different sources into electric energy to be stored and used later. These sources can be found in the environment or in the human body. Energy from the environment can be motion, thermal gradients, and RF^[4,5] and the energy from the human body can be in the form

of heat, biochemical and biomechanical, and it is more predictable.^[4] Biomechanical energy is attractive for wearable systems considering the dynamic nature of the human body. However, most of the sensors developed to harvest this kind of energy are more efficient at high frequencies and low displacements.^[6] However, in daily life, the dynamic of the human body is low frequency, random, and with large movements.^[7,8]

EH from the human motion captures the biomechanical energy from different activities that involve center of mass motion, joints motion, foot strike, and limb swing motion.^[9] More recently, efforts have been made to harvest energy, while the subject is doing daily activities such as using a computer, a smartphone, or even eating.^[7,10–13] In that sense, designing a wearable energy harvester becomes more challenging due to the strict physical constraints of wearable systems in terms of size, weight, form, and, in the case of clothing, mechanical flexibility.

Piezoelectric EH has been demonstrated to be an excellent technique for self-powered wearable systems.^[14] Commonly, polymer-based, flexible materials, such as PVDF, rather than rigid and brittle ceramics, such as lead zirconate titanate (PZT), are used.^[15] However, as the electrical energy obtained with PVDF sensors is low, intermittent operation with low duty cycle becomes mandatory.^[16] This problem has been tackled using power management circuits (PMCs) to accumulate energy in a storage device and then deliver it to the load. In that case, the load not only receives a regulated voltage intermittently but must deal with under-voltage conditions and avoids problems such as the lock-up phenomenon described in other works.^[17,18]

In this article, a self-powered glove-type wearable system is proposed to harvest and manage the energy from finger motion. To convert the biomechanical energy into electrical, five piezoelectric films sensors are used. The electrical energy is first conditioned and stored in a capacitor and then is delivered to the load. For this, a battery-less PMC is proposed to isolate the capacitor from the load during the charging phase, whereas the current consumption of the circuit is reduced. Once the level of energy reaches the requirements of a low-dropout linear voltage regulator (VR), the user decides when to transfer the stored energy to the load. In this work, the proposed system is tested by power supplying a cardiac pulse detection circuit. A similar piezoelectric glove has been already proposed by Psoma et al.,^[10] where the

O. Mendez-Lira, R. Gonzalez-Landaeta
Electrical and Computing Engineering Department
Autonomous University of Ciudad Juarez
Ciudad Juarez CH 32310, Mexico
E-mail: rafael.gonzalez@uacj.mx

E. M. Spinelli
GIBIC, LEICI Institute, Engineering School
National University of La Plata -CONICET
La Plata BA 1900, Argentina

The ORCID identification number(s) for the author(s) of this article can be found under <https://doi.org/10.1002/ente.202100520>.

DOI: 10.1002/ente.202100520

1 harvested energy was used to charge a nickel–metal hydride
2 (NiMH) battery from the impact of the fingers over a surface
3 using piezoelectric sensors located at the fingertips. This
4 approach can be obstructive and uncomfortable when using a
5 keyboard, computer mouse, a cellular phone, or a tablet. The sys-
6 tem herein proposed is unobtrusive and user friendly.

7 The manuscript is organized as follows. Section 2 describes
8 the EH principle each stage of the energy-conditioning system.
9 Section 3 explains the work principle of the proposed battery-less
10 PMC and analyzes the effect of the circuit losses. Section 4
11 describes the battery-less circuit used to detect the cardiac pulse.
12 Section 5 describes the setups and the measurements to charac-
13 terize the energy harvesters and the energy-conditioning circuit.
14 Section 6 presents and discusses the results and Section 7 draws
15 the main conclusions.

16 2. EH and Conditioning

17 The proposed system harvests the energy produced by the finger
18 motion. For this, five PVDF film-type piezoelectric sensors (piezo-
19 films) are mounted in a glove-type garment. As the subject puts it
20 on, the piezofilms match different interphalangeal joints of the fin-
21 gers to generate higher voltages, while the subject moves his/her
22 fingers.^[19] The sensors are placed on the posterior-proximal inter-
23 phalangeal joint of the thumb and the posterior-proximal interpha-
24 langeal junctions of each of the other four fingers. With this
25 distribution, the sensors do not generate voltage from impacts
26 but rather from the movements of each finger.

27 The movements of the fingers are low frequency, high ampli-
28 tude, and random, so the generated voltage from the harvesting
29 sensors is not suitable to power an electronic circuit continu-
30 ously. **Figure 1** shows the proposed circuit for conditioning
31 and managing the energy harvested by the piezoelectric sensors.

32 The generated voltage is full-wave rectified by a rectifier bridge
33 implemented with diodes with low-forward voltage and low-
34 leakage currents, which are the main sources of power loss.^[20]
35 An over-voltage protection is placed to prevent the storage capac-
36 itor and the VR from being damaged when the energy is still
37 being harvested and the system does not deliver the energy to
38 the load. For this, a Zener diode, D_Z , with a voltage, V_Z , is used.

A diode, D , is placed between D_Z and the capacitor to reduce
the current losses because of the leakage currents of D_Z and the
rectifier bridge. The combination of D_Z and D makes the maxi-
mum voltage across C , V_{C_max} , not exceed the maximum input
voltage of VR, V_{IN_max} . A capacitor C is used as the energy-
storage device; its value should not be so high to shorten the
charging time, nor so low to maintain the stored voltage for long-
er; this trade-off will be discussed in the following subsections.
 C must have a high insulating resistance to maintain the har-
vested energy longer when no energy is harvested. Although
capacitors are not recommended as storage devices when energy
is harvested from limb motions (walking or typing),^[21] this work
shows that good management of the harvested energy makes the
capacitor a suitable option for battery-less applications.

3. Power Management Circuit

The proposed PMC is a battery-less circuit that alternates
between an energy-storage phase and an energy-delivery phase.
During the former, C is isolated from the load while being
charged using the energy harvested from the fingers. During
the latter, the stored energy is transferred to the load, making
 C discharge gradually. The energy-delivery phase lasts until
the stored voltage reaches a low threshold voltage, V_L . In our
case, the user decides when to power the load, but first, C must
reach a high threshold voltage V_H . Both threshold voltages must
be adjusted between the allowable voltage range of the VR, that is,
 $V_{IN_min} \leq V_L < V_H \leq V_{IN_max}$, $V_{IN_min} = V_{CC} + V_{DO}$, where V_{CC}
is the regulated output voltage, V_{DO} is the dropout voltage, and
 V_{IN_in} is the minimum input voltage at which VR begins to regu-
late, respectively.

A low-dropout and linear VR with a built-in ON/OFF circuit is
used to deliver a steady and regulated voltage to the load.
Although linear regulators are less efficient than switching ones,
the former are simpler to use, low cost, have low noise, and have
no AC switching losses.^[22] In the system proposed here, when
VR is off, C is isolated from the load; when VR is on, the stored
voltage in C is transferred to the load. The ON/OFF control is
achieved by two voltage dividers (R_1-R_2 and R_3-R_4), an opera-
tional amplifier (OA1) configured as a voltage comparator, and a

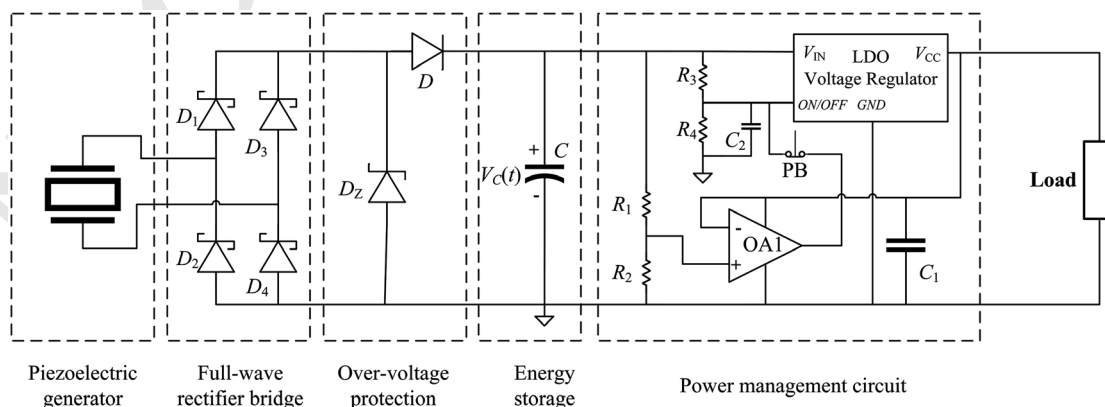


Figure 1. Proposed EH, conditioning, and PMC.

1 normally closed push button (PB), which opens when pressed
2 and closes when released.
3 In EH systems, PMCs work by switching or triggering
4 between energy-storage and energy-delivery phases^[22,23] but
5 under certain conditions, usually threshold voltages and/or
6 load requirements,^[18] so the load is powered intermittently.
7 In this proposal, a different approach is used. First, consider-
8 ing C as initially discharged, $V_C(0) = V_{IN} = 0$ V. When VR is
9 off, the full-wave rectified voltage charges C , causing $V_C(t)$ and
10 V_{IN} to increase. As the output of VR is 0 V, OA1 is off. In this
11 case, the voltage divider formed by R_1 – R_2 is not involved with
12 the startup or shutdown of the system. The input current coming
13 from C finds a ground path through R_3 , PB, and the low
14 output resistance of OA1, making $V_{ON/OFF} = 0$ V, maintaining
15 VR off. Although $V_C(t) \geq V_{IN_min}$, VR is still off until PB is
16 pressed. The instant when PB is pressed, the ground path
17 of the input current is through R_3 and R_4 , and now
18 $V_{ON/OFF}$ is

$$Q4 \quad V_{ON/OFF} = V_C \frac{R_4}{R_3 + R_4} \quad (1)$$

19 Knowing the value of V_{ON} (minimum voltage of $V_{ON/OFF}$ to
20 activate VR), the values of R_3 and R_4 can be estimated for a
21 desired $V_C(t)$ ($= V_H$) that turns on VR when PB is pressed.
22 Assuming a high value of R_3 to reduce the current consumption,
23 R_4 can be obtained by

$$R_4 = \frac{V_{ON}}{V_C - V_{ON}} R_3 \quad (2)$$

24 Once PB is released, if $V_C(t) \geq V_H$, the VR output changes
25 from 0 V to V_{CC} due to the output of OA1, and the energy-
26 delivery phase begins. OA1 is configured as a voltage comparator;
27 whenever $V^+ > V^-$, $V_{ON/OFF}$ changes to V_{CC} and VR is on until
28 $V_C(t) = V_L$. At this point, R_1 and R_2 make $V^+ \leq V^-$, and the OA1
29 output and $V_{ON/OFF}$ change from V_{CC} to 0 V, turning off the VR
30 and stopping the energy delivery to the load. If PB is not released,
31 OA1 cannot control the state (on/off) of VR.

32 Assuming R_2 to be very high to reduce the current consump-
33 tion, for a given V_L ($= V_{IN_min}$), R_1 can be estimated by

$$R_1 = \frac{V_L - V^+}{V^+} R_2 \quad (3)$$

34 When VR is off, the current consumption is considerably
35 reduced, lowering the discharging rate of C . In Figure 1, C_1
36 reduces the ripple of the supply voltage of OA1 and C_2 reduces
37 the ripple of V_{CC} when PB is pressed and released.

38 3.1. Energy Storage

39 For the analysis presented here, we have considered the equiva-
40 lent circuit shown in Figure 2a for each piezoelectric sensor.^[16]

41 In our case, the output signal of the piezoelectric sensors is
42 full-wave rectified (Figure 2b) instead of using a voltage doubler.
43 Considering just one piezoelectric sensor in Figure 2b, C_s , which
44 is the output capacitance of the sensor, is discharged/recharged
45 in an opposite way each semicycle, and this charge is accumu-
46 lated in C at each semicycle of the input signal. Considering the

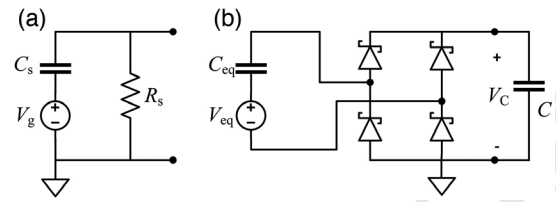


Figure 2. A) Equivalent circuit of a single piezoelectric sensor and B) equivalent circuit when the five piezofilms are electrically interconnected in series and in parallel to charge C , with V_{eq} full-wave rectified.

electric charge conservation law, the charge stored in C (Q_C) at a
certain k -semiperiod, $k > 0$, is

$$Q_C(k) = Q_{Cs}(k) + Q_C(k-1) + Q_{Cs}(k-1) \quad (4)$$

$$CV_C(k) = C_s(V_p - V_C(k)) + CV_C(k-1) + C_s(V_p - V_C(k-1)) \quad (5)$$

Rearranging

$$V_C(k) = 2V_p \left(\frac{C_s}{C_s + C} \right) + V_C(k-1) \left(\frac{C - C_s}{C_s + C} \right) \quad (6)$$

Solving the discrete difference in Equation (6), considering
 $V_C(0) = 0$, $V_C(1) = V_p C_s / (C_s + C)$, and the forward voltage of
the rectifier diodes (V_γ), the voltage across C as a function of
 k -semiperiod, results in

$$V_C(k) = (V_p - 2V_\gamma) \left[1 - \frac{C}{C - C_s} \left(\frac{C - C_s}{C_s + C} \right)^k \right]; k \geq 1 \quad (7)$$

where V_p is the peak amplitude of the input voltage. Using a full-
wave rectifier, C charges twice per each cycle of the input signal,
so, $k = 2t/T = 2tf$, f being the frequency of the input signal and t
time. Now, the voltage across C as function of time and
frequency is

$$V_C(t, f) = (V_p - 2V_\gamma) \left[1 - \frac{C}{C - C_s} \left(\frac{C - C_s}{C_s + C} \right)^{2tf} \right] \quad (8)$$

Considering $V_C(0) \neq 0$ and $C \gg C_s$, Equation (8) can be
rewritten as

$$V_C(t, f) \approx V_p \left[1 - \left(1 - \frac{V_C(0)}{V_p} \right) (1 - 2C_s/C)^{2tf} \right] \quad (9)$$

and the time needed for C to reach a given voltage V_x can be
estimated by

$$t \approx \frac{C}{4fC_s} \ln \left(\frac{(V_p - 2V_\gamma) - V_C(0)}{(V_p - 2V_\gamma) - V_x} \right) \quad (10)$$

Although a high value of C would maintain the stored voltage
for longer, it also implies that it would take a longer time to reach
 V_H . Hence, from Equation (10), some scenarios can be considered
to reach V_H faster: 1) using an initially charged C , 2) increasing
 C_s , 3) increasing V_p , and 4) increasing the frequency of the
deformations. Scenario (1) can be achieved by making $V_C(0) > 0$

1 once the energy-delivery phase concludes. Scenario (4) is quite
2 difficult to control because of the randomness of the movements.
3 Nevertheless, Scenarios (2) and (3) are more predictable because
4 the value of C_s and V_p can be determined by interconnecting the
5 piezoelectric sensors in series or in parallel. However, it is
6 necessary to assess which is the best option, because the effects
7 on C_s and V_p are opposites.

8 In our proposal, each piezofilm harvests energy from the
9 movements of each finger independently, so the harvested
10 energy varies from sensor to sensor. Figure 2b shows the equiv-
11 alent circuit when the sensors are interconnected either in series
12 or in parallel to charge C , where R_s of Figure 2a has been
13 disregarded due to its very high value.

14 Considering five identical sensors, in series, the total open-
15 circuit voltage is the sum of the voltages generated by each sensor
16 ($V_{eq} = 5 V_g$) and $C_{eq} = C_s/5$. In parallel, the total voltage is the
17 same of one sensor ($V_{eq} = V_g$) and $C_{eq} = 5C_s$. Considering the
18 peak amplitude (V_p) of the open-circuit voltage of each sensor,
19 from Equation (9), considering $V_C(0) \neq 0$, $V_C(t,f)$ for each topol-
20 ogy is defined by

21 Series

$$V_C(t,f) \approx (5V_p - 2V_\gamma) \left[1 - \left(1 - \frac{V_C(0)}{5V_p} \right) (1 - 2C_s/(5C))^{2ft} \right] \quad (11)$$

22 Parallel

$$V_C(t,f) \approx (V_p - 2V_\gamma) \left[1 - \left(1 - \frac{V_C(0)}{V_p} \right) (1 - 2(5C_s)/C)^{2ft} \right] \quad (12)$$

23 For $t \rightarrow \infty$, it is obvious the series topology achieves $V_C = 5 V_p$,
24 approximately; so, at first instance, it is the best choice if C needs
25 to be charged to a higher voltage. However, in the system pro-
26 posed here, the PMC and the load only need +2 V, and it is not
27 necessary for $V_C(t)$ to reach $5 V_p$; otherwise, a lot of power will be
28 lost due to the difference between V_{IN} and V_{out} of VR.
29 Preliminary tests show that opening and closing the hand make
30 each sensor provides 37 V, approximately. From Equation (10),
31 considering V_x between 2 V and 5 V, the parallel topology is
32 the best option to make C reach V_H faster.

33 Once $V_C(t)$ is estimated, the energy storage in C (E_C) can be
34 obtained by

$$E_C = \frac{1}{2} C (V_{Cmax}^2 - V_{Cmin}^2) \text{ (Joules)} \quad (13)$$

35 where V_{Cmax} and V_{Cmin} are the maximum and minimum voltage
36 across C , respectively.

37 3.2. Circuit Losses and Energy Delivery

38 **Figure 3** shows the equivalent circuit of the system of Figure 1,
39 where the current loads and the equivalent resistances seen from
40 C are presented. From this circuit, it is possible to estimate the
41 discharge rate when the load is isolated from C and when the
42 stored voltage is delivered to the load.

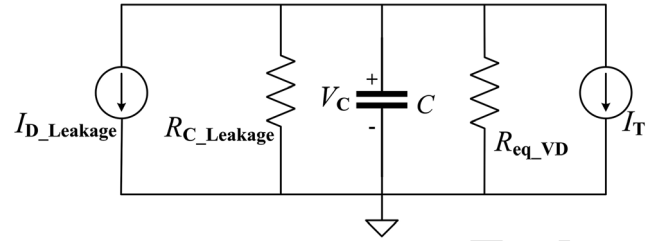


Figure 3. Equivalent circuit of the system of Figure 1 that shows the cur-
rent loads and the equivalent resistances seen from C .

From Figure 3, $V_C(t)$ can be estimated by

$$V_C(t) = V_C(0)e^{-t/R_{eq}C} + IR_{eq}(e^{-t/R_{eq}C} - 1) \quad (14)$$

where $V_C(0)$ is the initial voltage across C , R_{eq} ($R_{C_Leakage} || R_{eq_VD}$)
is the equivalent resistance, which depends on the insulating
resistance of C , $R_{C_Leakage}$, and the equivalent resistance of the
two voltage dividers, R_{eq_VD} , and I is the current consumption
of the entire circuit, which depends on the state of VR. For
 $t \ll R_{eq}C$, $V_C(t)$ is

$$V_C(t) \approx V_C(0) - (V_C(0) + IR_{eq})t/R_{eq}C \quad (15)$$

From Equation (15), the discharge rate of C can be approximated
as linear. When VR is off, C discharges due to the current through
the resistors R_1 , R_2 , R_3 , R_4 , and $I_{D_leakage}$ (the reverse current of D).
If $I_{D_Leakage}$ is very low, $V_C(t)$ depends mainly on $V_C(0) - V_C(0)t/
R_{eq}C$. By making R_{eq} large, the discharge of C will be slower.
When VR is on, the current drawn by VR and the load dominates,
and $V_C(t)$ depends on $V_C(0) - It/C$, with $I \approx I_T \approx I_{VR_ON} + I_{LOAD}$,
where I_{VR_ON} is the current consumption when VR is on, and I_{LOAD}
is the current consumption of the circuits of **Figure 4**. In this sce-
nario, C discharges faster and the autonomy of the system depends
on the time it takes C to reach V_L . The leakage currents of D_Z and
the rectifier bridge are considered negligible because these diodes
work at a voltage close to 0 V. This is because when D is reverse
biased and D_Z is off, D acts as an open circuit, causing a large volt-
age drop between the cathode and the anode of D.

4. The Load

The load of the system of Figure 2 is the battery-less cardiac pulse
detection circuit of Figure 4a, the voltage reference circuit of
Figure 4b, and a Transflective Polarizer LCD Display with no
backlight. In Figure 4a, when the cardiac sensor (piezoelectric
sensor) detects the cardiac pulse, the output voltage of the sensor
is amplified by a noninverting amplifier with gain $G = 1 + (R_B/
R_A)$. R_x and the output capacitance of the cardiac sensor
(C_{sensor}) define the time constant ($\tau = C_{sensor}R_x$) and the high-
pass response of the system, which must be able to detect the
cardiac pulse. A first-order passive low-pass filter formed by
 C_F and R_F reduces the noise bandwidth and the contribution
of some electromagnetic interferences. The reference voltage
of the circuit of Figure 4a is set to $V_{CC}/2$ using the system of
Figure 4b. Both circuits are powered by a regulated voltage
 V_{CC} provided by VR. The current consumption of the circuits

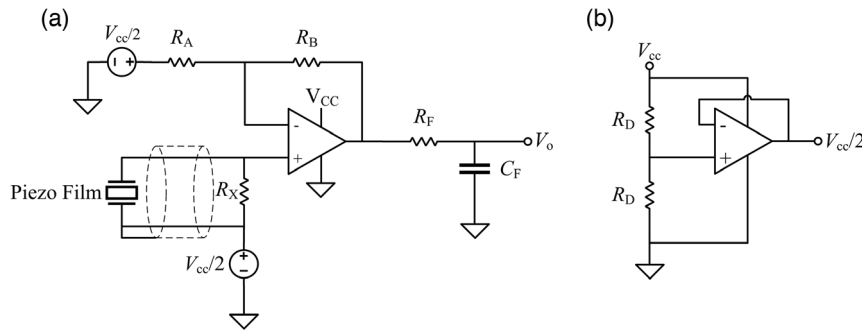


Figure 4. A) Cardiac pulse detection system and B) voltage reference circuit.

1 of Figure 4 depends on the quiescent current (I_Q) and the output
2 current (I_{out}) of each amplifier, namely, $I_{LOAD} \approx 2(I_Q + I_{out})$. The
3 circuit of Figure 4a draws more current because of the amplitude
4 of the cardiac signal. The LCD indicates if the harvesting system
5 is in the energy-storage phase (OFF) or in the energy-delivery
6 phase (ON). The current consumption of the LCD has been
7 neglected because it is quite lower than the op-amps.

8 5. Experimental Section

9 **Table 1** shows the components used in each stage of the circuit
10 shown in Figure 1 and their main characteristics, except the load.
11 To choose the optimal value of C , preliminary tests were made
12 with capacitors of 68 μF , 100 μF , 150 μF , and 1 mF. To achieve a
13 balance between both the energy-storage and energy-deliver
14 phases, a 68 μF capacitor was chosen to implement the system
15 of Figure 1 and conduct all the tests. The storage capacitor used
16 here was ceramic, because the electrolytic ones, commonly used
17 in this type of system,^[24,25] had a higher self-discharge rate.^[26] C
18 can support up to 25 V, which was higher than $V_{IN,max}$. However,
19 the combination of D_Z and D made V_C reach $V_Z - V_F$, protecting
20 C and VR. Maybe using a high-input voltage VR would avoid the
21 use of D_Z and D ; however, using high-input voltage VRs implies
22 that a higher voltage difference between input and output must
23 be considered, causing further loss of power.^[27]

24 To assess the effect of the electrical connection between all the
25 sensors, real conditions were tested. For this, five LDT1-028 K
26 from Measurement Specialties were mounted on a glove, which
27 was used by a volunteer. The volunteer was then asked to close
28 and open his/her hand following a 1 Hz and 2 Hz pattern during
29 20 s each. This experiment was conducted when the sensors were
30 interconnected both in series and in parallel. The total output
31 voltage of the five sensors was full-wave rectified to charge C ;
32 during this test, the circuit of Figure 2b was used, and $V_C(t)$
33 was measured using DAQ NI USB-6341 from National
34 Instruments.

35 To estimate R_1 and R_4 , we assumed $R_2 = R_3 = 100 \text{ M}\Omega$ to
36 reduce the current consumption. $V_H = +5 \text{ V}$, $V_L = +2.25 \text{ V}$,
37 and $V^+ = +1.99 \text{ V}$, which was enough to produce a change from
38 0 V to V_{CC} at the OA1 output. $V_{ON} \geq 0.63 \text{ V}$ and $V_{OFF} \leq 0.54 \text{ V}$.
39 These values were estimated experimentally, measuring $V_{ON/OFF}$
40 with a 6½-digit Digital Multimeter 34461 A from Keysight when
41 VR was turned on and off, respectively. From Equations (2) and

Table 1. Main characteristics of the components used to implement the system of Figure 1.

Stage	Item	Main Characteristics
Piezoelectric generator	LDT1-028 K	$C_s = 1.38 \text{ nF}$
Full-wave rectifier bridge	Schottky Diodes BAR28	$V_F = 0.41 \text{ V}$ $I_R = 200 \text{ nA @ } 50 \text{ V (max)}$
Overvoltage protection	Zener Diode BZX55C6V2-TA	$V_Z = 6.3 \text{ V (typ)}, 6.6 \text{ V (max)}$ $I_R < 100 \text{ nA @ } 2 \text{ V}$
	Small-Signal Diode 1N4151TAP	$V_F = 0.8 \text{ V (typ)}, 1 \text{ V (max)}$ $I_R = 50 \text{ nA @ } 50 \text{ V (max)}$
Energy storage	Capacitor	68 μF , 25 V, Ceramic.
PMC	Voltage Regulator S-1313B20-M5T1U3	$V_{IN(max)} = 6.0 \text{ V}^{\text{a}}$ $V_{CC} = 2 \text{ V (1.0\%)}$ $V_{DO} = 0.23 \text{ V (typ)}$
	Operational Amplifier MCP6041T-1/OT	Current consumption: ON: 1.35 $\mu\text{A @ } 3 \text{ V (no load)}$ OFF: 100 nA @ 3 V (no load) $I_Q = 1 \mu\text{A (max)}$
	Push Button	Normally closed
	R_1	13 M Ω , 1%
	R_2	100 M Ω , 5%
	R_3	100 M Ω , 5%
	R_4	13 M Ω + 1.6 M Ω , 5%
	C_1	100 nF, 25 V
	C_2	270 pF, 25 V

^a)Absolute maximum rating.

(3), $R_1 = 13.06 \text{ M}\Omega$ and $R_4 = 14.41 \text{ M}\Omega$. To implement the
1 circuit, we used commercial values of 13 M Ω for R_1 and a series
2 combination of 13 M Ω and 1.6 M Ω for R_4 .
3

4 In Figure 4a, a shielded piezoelectric sensor SDT1-028 K
5 ($C_s = 2.78 \text{ nF}$) from Measurement Specialties was used as the
6 cardiac sensor. The gain of the noninverting amplifier was 11
7 ($R_A = 1 \text{ M}\Omega$ and $R_B = 10 \text{ M}\Omega$), and the bandwidth, defined by
8 R_F and C_F , was 10 Hz. $R_x = 30 \text{ M}\Omega$, so $\tau = 83.4 \text{ ms}$. In
9 Figure 4b, $R_D = 10 \text{ M}\Omega$ to reduce the current consumption.
10 The op-amp used in both circuits was TLV522DGK from 10

1 Texas Instruments, which was a dual-nanopower amplifier,
2 where each op-amp had a quiescent current $I_Q = 800$ nA
3 (max), a wide supply range (from +1.7 V to +5 V), and a very
4 high input impedance ($10^{13} \Omega \parallel 2.5$ pF). Both circuits were powered
5 at +2.0 V provided by the low-dropout VR S-1313D22-
6 M5T1U3 from ABLIC.

7 The measurement setup shown in **Figure 5** was used to conduct
8 two tests, where C was initially charged to +5.15 V using a
9 DC power supply E3631A from Keysight (not shown in the figure).
10 In the first test, $V_C(t)$ was measured, whereas VR was off;
11 the discharging rate was estimated when no energy was

transferred to the load. Then, $V_C(t)$ was measured when VR powered
1 the PMC and the load. During this part of the test, the cardiac
2 sensor was placed on the radial artery to detect the cardiac
3 pulse using the energy stored in C . In the second test, once $V_C(t)$
4 reached V_L and VR was turned off, the volunteer opened and
5 closed his/her hand to harvest energy, and the time needed
6 for $V_C(t)$ to reach V_H was estimated. During both tests, $V_C(t)$
7 was measured by a DAQ USB6341 from National
8 Instruments; the current consumption was estimated by
9 $I_{avg} = C\Delta V_C/t$, and E_C was estimated by Equation (13). 10

11 Finally, the same volunteer, wearing the glove, used a computer
12 (QWERTY keyboard and a mouse) and a cellular phone for 10 min
13 each, without any restrictions. For this test, VR was off, the five
14 piezofilms were interconnected in parallel, and all the stages of the
15 system of Figure 1 were connected to C , $V_C(t)$ was measured, and
16 E_C was estimated.

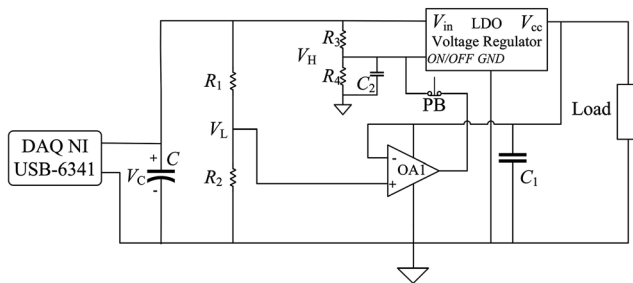


Figure 5. Experimental setup used to measure V_C when the VR was off and on.

6. Results and Discussion

Figure 6 shows the open-circuit voltage (V_{eq}) of the five piezofilms
18 connected in parallel (Figure 6a) and in series (Figure 6b), when the
19 volunteer opened and closed his/her hand at 2 Hz using the glove.
20 First, a nonperfect and nonsymmetric sinusoidal wave from finger
21 movement is shown. Second, $V_{p_parallel} \approx 5 V_{p_series}$, that is, 36 V 22

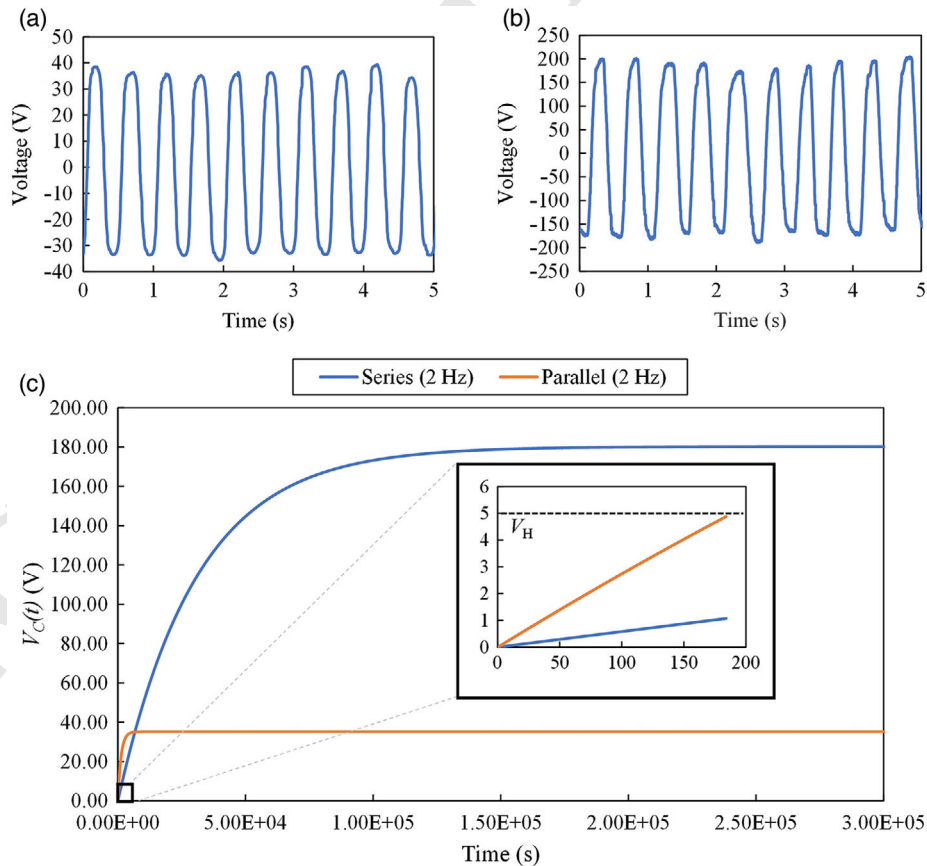


Figure 6. Open-circuit voltage of the five sensors when the subject opened and closed his hand at 2 Hz wearing the glove. A) Sensors interconnected in parallel and B) in series. C) Theoretical results of $V_C(t)$ during 300×10^3 s using both topologies.

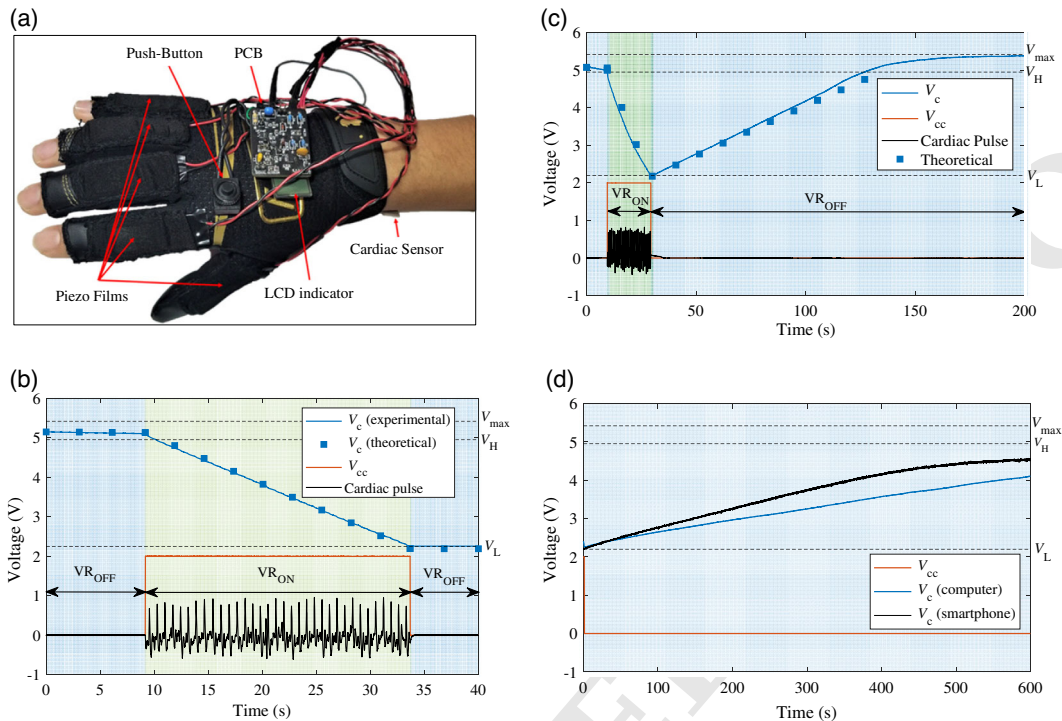


Figure 7. A) Photograph of the wearable system that harvests biomechanical energy to power a battery-less cardiac pulse detection circuit, B) voltage across C when VR is turned on and off, C) performance of the system when the energy is harvested as the subject opened and closed the hand at 2 Hz, approximately, and D) $V_C(t)$ (while VR was off) using the biomechanical energy of the fingers when the subject, wearing the glove, used a computer (keyboard and mouse) and cellular phone for 10 min each.

1 (parallel) and 181 V (series), approximately, making the series topol-
2 ogy the best option to generate higher voltages. Figure 6c shows the
3 theoretical results obtained from Equations (11a) and (11b), where
4 $C = 68 \mu\text{F}$, $C_s = 1.38 \text{ nF}$, $V_\gamma = 0.4 \text{ V}$, and $t = 300 \times 10^3 \text{ s}$. $V_C(t)$
5 reaches almost 181 V for the series topology and 36 V for the parallel
6 topology. However, these levels are never reached because of D_Z of
7 Figure 1. From the zoomed trace of Figure 6c, C reaches V_H faster
8 using the parallel topology. From Equation (10), when $V_C(0) = 0$,
9 the time needed for C to reach $V_H = +5 \text{ V}$ is 847.5 s, using the
10 series topology, and 183.1 s, using the parallel topology. When
11 $V_C(0) = +2.23 \text{ V}$, these times are reduced to 483.4 s and 108.1
12 s, respectively. In our case, the parallel topology is the best option,
13 because the priority is that C reaches V_H faster, not reaching a
14 higher voltage.

15 The proposed wearable system and its performance are shown
16 in Figure 7. The energy-conditioning system, the PMC, and the
17 circuits of Figure 4 were all included in the printed circuit board
18 (PCB) (Figure 7a). Figure 7b shows the performance of the sys-
19 tem, where C was initially charged to +5.15 V. While VR was off,
20 C discharged very slowly due to the low current ($\approx 103 \text{ nA}$) sunk
21 by $R_1 - R_4$ and due to $I_{D_leakage}$. When VR was turned on, +2 V
22 was supplied to the load, and the current consumption
23 ($= C \cdot \Delta V_C / t$) increased to $8 \mu\text{A}$ until $V_C(t)$ reached V_L
24 ($= 2.23 \text{ V}$); the main contribution to this “high” current was due
25 to I_{LOAD} and the current consumption of VR. C discharged faster
26 because of this high current; even so, it was enough to maintain the
27 autonomy of the PMC and the load for more than 20 s. During this

time, the cardiac pulse signal was clearly obtained. Once $V_C(t)$ 1
reached V_L , VR turned off, and the current consumption 2
decreased again. The theoretical results were obtained from 3
Equation (15), using $V_C(0) = +5.15 \text{ V}$, $C = 68 \mu\text{F}$, $R_{eq} = 45 \text{ M}\Omega$, 4
 $R_{eq_VD} = 57 \text{ M}\Omega$, and $R_{C_Leakage} \approx 200 \text{ M}\Omega$. 5

Figure 7c shows what happened when $V_C(t)$ reached V_L , and 6
then the volunteer wearing the glove closed and opened the hand 7
at 2 Hz; the five sensors were interconnected in parallel. When 8
VR turned off, $V_C(t)$ was at +2.25 V. Assuming this voltage as 9
 $V_C(0)$, from Equation (10), the time needed to reach V_H was 10
about 104 s, and the energy stored in C was about 850 μJ . 11
The experimental results validate Equations (12) and (15). 12

Figure 7d shows how C was charged from the finger motions 13
when the subject used a computer and a cellular phone for 14
10 min each. VR was off. When the volunteer used the computer 15
keyboard and mouse, the charging current was about 195 nA, $V_C(t)$ 16
reached +4.2 V, and, according to Equation (12), the stored energy 17
was about 580 μJ . When the subject used the cellular phone, the 18
charging current was 221 nA, $V_C(t)$ reached +4.5 V, and 700 μJ 19
was stored. It is evident that under these conditions, C needed more 20
time to reach V_H because the movement of the fingers is not as 21
large as opening and closing the hand at a fixed frequency. 22

7. Conclusion

A self-powered wearable system that harvests and manages the 24
biomechanical energy of the fingers was proposed. Five PVDF 25

1 film-type sensors mounted on a glove-type garment were used to
2 harvest the energy from finger movement, not the impact on a
3 surface. The harvested energy was conditioned and stored in a
4 68 μF ceramic capacitor. This energy was used to power for 20 s
5 a battery-less PMC and a battery-less circuit that detects the car-
6 diac pulse of the subject. The PMC was designed to isolate the
7 capacitor from the load to reduce the current consumption while
8 charging. Once the voltage across C reaches a high threshold volt-
9 age, the user controlled the energy delivery to the load. From
10 daily activities like using a computer/laptop or a cellular phone
11 for 10 min, it was possible to store up to 700 μJ in the capacitor.
12 Nevertheless, the proposed wearable system is not limited to the
13 activities presented here, because it can harvest the biomechanical
14 energy from any activity in which finger movements are
15 involved.

16 Supporting Information

17 Supporting Information is available from the Wiley Online Library or from
18 the author.

19 Conflict of Interest

20 The authors declare no conflict of interest.

21 Data Availability Statement

22 Research data are not shared.

23 Keywords

24 battery less, biomechanical energy, energy harvesting, power management
25 circuits, wearable systems

26 Received: June 14, 2021

27 Revised: August 1, 2021

28 Published online:

- 29 [1] Y. Zou, V. Raveendran, J. Chen, *Nano Energy* **2020**, *77*, 105303.
30 [2] J. Chen, Y. Huang, N. Zhang, H. Zou, R. Liu, C. Tao, F. Xing,
31 Z. L. Wang, *Nat. Energy* **2016**, *1*, 1.

- [3] M. Magno, D. Boyle, in *Proc. 12th Int. Conf. on Design & Technology of Integrated Systems In Nanoscale Era (DTIS)* (Eds: E. Isern, M. Roca, T. Margaria), Palma de Mallorca, Spain **2017**. 1
2
3
[4] Y.-W. Chong, W. Ismail, K. Ko, C.-Y. Lee, *IEEE Sens. J.* **2019**, *19*, 9047. 4
[5] S. Beeby, N. M. White, *Energy harvesting for autonomous systems*, Artech House, Norwood, MA **2010**. 5
6
[6] P. D. Mitcheson, E. M. Yeatman, G. K. Rao, A. S. Holmes, T. C. Green, *Proc. IEEE*. **2008**, *96*, 1457. 7
8
[7] Q. Cheng, Z. Peng, J. Lin, S. Li, F. Wang, *presented at 10th IEEE Inter. Conf. on Nano/Micro Engineered and Molecular Systems*, Xi'an, April 2015. 9
10
[8] W.-S. Jung, M.-J. Lee, M.-G. Kang, H. G. Moon, S.-J. Yoon, S.-H. Baek, C.-Y. Kang, *Nano Energy* **2015**, *13*, 174. 11
12
[9] M. Cai, Z. Yang, J. Cao, W.-H. Liao, *Energ. Tech.* **2020**, *8*, 2000533. 13
14
[10] S. Psoma, P. Tzanetis, A. Tourlidakis, *Mater. Today: Proc.* **2017**, *4*, 6771. 15
16
[11] G. De Pasquale, S.-G. Kim, D. De Pasquale, *IEEE/ASME Trans. Mechatron.* **2015**, *21*, 565. 17
18
[12] Y. Cha, J. Hong, J. Lee, J.-M. Park, K. Kim, *Sensors* **2016**, *16*, 1045. 19
[13] A. Delnavaz, J. Voix, *Smart Mater. Struct.* **2014**, *23*, 105020. 20
[14] Y. Liu, H. Khanbareh, M. A. Halim, A. Feeney, X. Zhang, H. Heidari, R. Ghannam, *Nano Select*, **2021**, *1*. 21
22
[15] Y.-M. Choi, M. G. Lee, Y. Jeon, *Energies* **2017**, *10*, 1483. 23
[16] M. Ferrari, V. Ferrari, M. Guizzetti, D. Marioli, *Smart Mater. Struct.* **2009**, *18*, 085023. 24
25
[17] B. H. Stark, G. D. Szarka, E. D. Rooke, *IET Circuits Devices Syst.* **2011**, *5*, 267. 26
27
[18] D. Alghisi, V. Ferrari, M. Ferrari, F. Touati, D. Crescini, A. Mnaouer, *Sens. Actuators, A* **2017**, *263*, 305. 28
29
[19] O. Méndez-Lira, E. Sifuentes, R. González-Landaeta, in *Proc. 2019 Latin American Conference on Biomedical Engineering* (Eds: C. González, Ch. Chapa, E. Laciari, H. Velez, N. Puente, D.-L. Flores, A. Andrade, H. Galván, F. Martínez, R. García, C. Trujillo, A. Mejía), Cancun, Mexico **2016**. 30
31
[20] G. D. Szarka, B. H. Stark, S. G. Burrow, *IEEE Trans. Power Electron.* **2011**, *27*, 803. 32
33
[21] T. Starner, J. A. Paradiso, *Low-Pow. Electron. Desig.* **2004**, *45*, 1. 34
35
[22] D. Alghisi, V. Ferrari, M. Ferrari, D. Crescini, F. Touati, A. Mnaouer, *Sens. Actuators, A* **2017**, *264*, 234. 36
37
[23] D. Marinkovic, A. Frey, I. Kuehne, G. Scholl, *Proc. Chem.* **2009**, *1*, 1447. 38
39
[24] T. Starner, *IBM Syst. J.* **1996**, *35*, 618. 40
41
[25] M. Guan, W.-H. Liao, *J. Intell. Mater. Syst. Struct.* **2008**, *19*, 671. 42
43
[26] R. L. Boylestad, *Introductory Circuit Analysis*, Pearson Education, London, UK **2016**. 44
45
[27] G. Morita, *Analog Dialogue* **2014**, *48*, 1. 46

